Dynamic stereo microscopy for studying particle sedimentation

M. P. Lee,[1,*] G. M. Gibson,[1] D. Phillips,[1] M. J. Padgett,[1] and M. Tassieri[2]

[1]*School of Physics and Astronomy, SUPA, University of Glasgow, G12 8QQ, UK*
[2]*Division of Biomedical Engineering, School of Engineering, University of Glasgow, G12 8LT, UK*
[*]*m.lee.2@research.gla.ac.uk*

Abstract: We demonstrate a new method for measuring the sedimentation of a single colloidal bead by using a combination of optical tweezers and a stereo microscope based on a spatial light modulator. We use optical tweezers to raise a micron-sized silica bead to a fixed height and then release it to observe its 3D motion while it sediments under gravity. This experimental procedure provides two independent measurements of bead diameter and a measure of Faxén's correction, where the motion changes due to presence of the boundary.

OCIS codes: (350.4855) Optical tweezers or optical manipulation; (230.6120) Spatial light modulators; (150.6910) Three-dimensional sensing.

References and links

1. C. Maurer, A. Jesacher, S. Bernet, and M. Ritsch-Marte, "What spatial light modulators can do for optical microscopy," Laser Photonics **5**(1), 81–101 (2011).
2. Z. Wang, L. Millet, M. Mir, H. Ding, S. Unarunotai, J. Rogers, M. U. Gillette, and G. Popescu, "Spatial light interference microscopy (SLIM)," Opt. Express **19**(2), 1016–1026 (2011).
3. S. Bernet, A. Jesacher, S. Fürhapter, C. Maurer, and M. Ritsch-Marte, "Quantitative imaging of complex samples by spiral phase contrast microscopy," Opt. Express **14**(9), 3792–3805 (2006).
4. S. R. P. Pavani and R. Piestun, "Three dimensional tracking of fluorescent microparticles using a photon-limited double-helix response system," Opt. Express **16**(26), 22048–22057 (2008).
5. J. S. Dam, I. R. Perch-Nielsen, D. Palima, and J. Glückstad, "Three-dimensional imaging in three-dimensional optical multi-beam micromanipulation," Opt. Express **16**(10), 7244–7250 (2008).
6. R. Bowman, D. Preece, G. Gibson, and M. Padgett, "Stereoscopic particle tracking for 3D touch, vision and closed-loop control in optical tweezers," J. Opt. **13**(4), 044003 (2011).
7. M. Lee, G. Gibson, R. Bowman, S. Bernet, M. Ritsch-Marte, D. Phillips, and M. Padgett, "A multi-modal stereo microscope based on a spatial light modulator," Opt. Express **21**(14), 16541–16551 (2013).
8. S. Quirin, D. S. Peterka, and R. Yuste, "Instantaneous three-dimensional sensing using spatial light modulator illumination with extended depth of field imaging," Opt. Express **21**(13), 16007–16021 (2013).
9. G. Leitz, B.-H. Kang, M. E. Schoenwaelder, and L. A. Staehelin, "Statolith sedimentation kinetics and force transduction to the cortical endoplasmic reticulum in gravity-sensing arabidopsis columella cells," Plant Cell **21**(3), 843–860 (2009).
10. S. Heitkam, Y. Yoshitake, F. Toquet, D. Langevin, and A. Salonen, "Speeding up of sedimentation under confinement," Phys. Rev. Lett. **110**(17), 178302 (2013).
11. R. Blazejewski, "Apparent viscosity and settling velocity of suspensions of rigid monosized spheres in stokes flow," Int. J. Multiphase Flow. **39**, 179–185 (2012).
12. J. Palacci, C. Cottin-Bizonne, C. Ybert, and L. Bocquet, "Sedimentation and effective temperature of active colloidal suspensions," Phys. Rev. Lett. **105**(8), 088304 (2010).
13. A. T. Juhl, D.-K. Yang, V. P. Tondiglia, L. V. Natarajan, T. J. White, and T. J. Bunning, "Ordering of glass rods in nematic and cholesteric liquid crystals," Opt. Mater. Express **1**(8), 1536–1547 (2011).

#203463 - $15.00 USD Received 19 Dec 2013; revised 6 Feb 2014; accepted 8 Feb 2014; published 20 Feb 2014

14. A. Ashkin, J. Dziedzic, J. Bjorkholm, and S. Chu, "Observation of a single-beam gradient force optical trap for dielectric particles," Opt. Lett. **11**(5), 288–290 (1986).
15. A. Yao, M. Tassieri, M. Padgett, and J. Cooper, "Microrheology with optical tweezers," Lab Chip **9**(17), 2568–2575 (2009).
16. M. Tassieri, R. Evans, R. L. Warren, N. J. Bailey, and J. M. Cooper, "Microrheology with optical tweezers: data analysis," New J. Phys. **14**(11), 115032 (2012).
17. G. M. Gibson, J. Leach, S. Keen, A. J. Wright, and M. J. Padgett, "Measuring the accuracy of particle position and force in optical tweezers using high-speed video microscopy," Opt. Express **16**(19), 14561–14570 (2008).
18. M. Hasler, T. Haist, and W. Osten, "Stereo vision in spatial-light-modulator–based microscopy," Opt. Lett. **37**(12), 2238–2240 (2012).
19. R. W. Bowman, G. M. Gibson, A. Linnenberger, D. B. Phillips, J. A. Grieve, D. M. Carberry, S. Serati, M. J. Miles, and M. J. Padgett, "Red tweezers: Fast, customisable hologram generation for optical tweezers," Comput. Phys. Commun. **185**(1), 268 (2014).
20. C. Gosse and V. Croquette, "Magnetic tweezers: micromanipulation and force measurement at the molecular level," Biophys. J. **82**(6), 3314–3329 (2002).
21. X. Michalet, "Mean square displacement analysis of single-particle trajectories with localization error: Brownian motion in an isotropic medium," Phys. Rev. E **82**(4), 041914 (2010).

1. Introduction

The use of Spatial Light Modulators (SLMs) in microscopy allows the interactive control of the image Point Spread Function (PSF) [1]. This is achieved by placing the SLM in the Fourier plane of the sample, where a phase pattern can be applied to the spatial frequencies of the image. Both the phase and the amplitude of light can be modified by displaying the appropriate pattern on the SLM, such that classical microscopy techniques, like phase contrast and darkfield microscopy, can be performed. In recent years, the versatility of SLMs has allowed new forms of microscopy to be developed [2–4].

In this work, we adopt a Fourier filter that changes in real time, based on information obtained from images taken by a camera. In particular, we use a SLM based stereo microscope [5, 6] to measure the sedimentation of a silica bead immersed in water. The experimental configuration is such that the sedimenting bead falls towards the inverted microscope objective. We record the bead's 3D position over 10's μm *via* a stereo video particle tracking procedure. The bead position is used to continually update the focal power of a Fresnel lens on the SLM, so that the bead is always in focus. This extends the range of the procedure beyond the depth of field of standard microscopes [7], yet does not require computational deconvolution [8].

In absence of external flow and at low volume fractions, the bead's sedimentation is governed only by the balance between two body forces and one surface force, respectively, the gravity force ($\rho_s V_s g$), the buoyancy force ($\rho_f V_s g$), and the viscous force ($6\pi r\eta \frac{dz}{dt}$):

$$\frac{\mathrm{dz}}{\mathrm{dt}} = \frac{2\mathrm{gr}^2(\rho_\mathrm{s} - \rho_\mathrm{f})}{9\eta}, \tag{1}$$

where dz/dt is the sedimentation rate, $\mathrm{V_s}$ is the bead's volume, g is the acceleration due to gravity, r is the bead's radius, ρ_s and ρ_f are, respectively, the density of the bead and of the fluid and η is the fluid viscosity (in this case a Newtonian fluid, i.e. a fluid with a constant viscosity). It is ubiquitous in nature, from river bed formation to direction sensing in the roots of plants [9]. Sedimentation is an active area of research, with applications in many industrial processes [10–12]. It can also be used as a tool to probe physical properties of complex fluids, such as liquid crystals [13].

In this work we demonstrate a new technique to measure sedimentation rates. We use Optical Tweezers (OT) [14] to trap and raise a silica bead above a microscope coverslip. Our OT work by tightly focusing a laser beam with an inverted microscope objective, which is also used to visualise the sample. The high intensity gradient of the focused beam generates a confining force on dielectric beads with higher refractive index than the surrounding medium, and stabilises

#203463 - $15.00 USD Received 19 Dec 2013; revised 6 Feb 2014; accepted 8 Feb 2014; published 20 Feb 2014

them just above the focal point of the beam. OT are established microrheology tools, where they are used to probe the fluid viscoelastic properties [15]. Microrheology techniques have the advantage of being applicable in confined volumes as well as requiring low quantities of the fluid under investigation. A typical microrheology experiment, using existing methods [16] would measure the thermal fluctuations of a bead trapped by OT and then apply statistical mechanics to those position data for determining the fluid viscoelastic properties.

The thermal fluctuations can be measured by using video particle tracking procedures, where the position of bead is calculated from the analysis of images recorded by a high speed camera [17]. Stereo microscopy [5,6] has recently been developed with the goal of measuring these thermal fluctuations in three dimensions. For stereo microscopy's implementation with OT, two light sources are positioned above the sample, illuminating it from two different angles. Under this illumination condition, we see a double image of a objects in the sample. The lateral displacement between the two images tells us information about the defocus of the image (e.g. for a perfectly in focus image, the two images would overlap with one another). Therefore, in order to perform three dimensional particle tracking, the light from the two illumination angles needs to be separated. This can be done in the Fourier plane with two blazed gratings displayed side by side on the SLM [18]. A holographic lens can be added to the grating so that objects can be refocused without any adjustment of the microscope optics [7].

2. Experiment

2.1. Experimental set up

Our experimental set up is similar to that described in Ref. [7] and is shown in Fig. 1(a). We use a sample of silica beads of mean radius, $r = 2.37\mu m$ from Bangs Lab Inc. diluted in distilled water. The sample is prepared in a welled microscope glass slide and sealed with a $150\mu m$ thick coverslip. We illuminate the sample with two optical fibres (acrylic, 1.5mm diameter) held at an angle of $\alpha = \pm 30^\circ$ to vertical in the $x-z$ plane. These fibres are positioned in a custom 3D printed mount about 2mm from the top of the slide. A drop of water between the fibres and slide gives brighter illumination. Each fibre is coupled to a high power red (637nm, 20nm bandwidth) LED light source (Luxeon Rebel). This light is filtered with a 636nm, 10nm bandwidth interference filter prior to the camera.

The objective is a Zeiss $63\times$, 1.2 NA water immersion lens which is mounted on a linear stage (LS-50-M, ASI) for focusing and positioning of the optical trap. The trapping laser is a 671nm DPSS laser from Changchun New Industries Optoelectronics Technology Co., Ltd. which has a maximum power output of 300mW. The beam is expanded and directed in to the back aperture of the objective. The expanded beam is slightly diverging such that the laser focus is $7\mu m$ above the image plane.

A polarising beam splitter is used to separate image light from the light of the trapping laser. An image of the sample is formed 2cm from the beam splitter and here we place an adjustable aperture to reduce the field of view. A Fourier lens images the back aperture of the objective on to a 512×512 SLM (Boulder Nonlinear Systems XY series). We can quickly update the filter by calculating the desired pattern on the graphics card [19]. Images are recorded with a Dalsa Genie GM1020 CMOS camera, which with a reduced region of interest, can capture images at 500Hz. We align the camera such that the apparent x motion, resulting from z displacement, corresponds to pixel rows. This allows a higher acquisition rate.

2.2. Procedure

In order to perform the measurement, we load a bead into the trap and position it $32\mu m$ above the coverslip. The laser is then switched off via USB control and the bead position recorded until it sediments onto the coverslip. We observe a small delay of 1.5 ± 0.1ms between the command

#203463 - $15.00 USD Received 19 Dec 2013; revised 6 Feb 2014; accepted 8 Feb 2014; published 20 Feb 2014

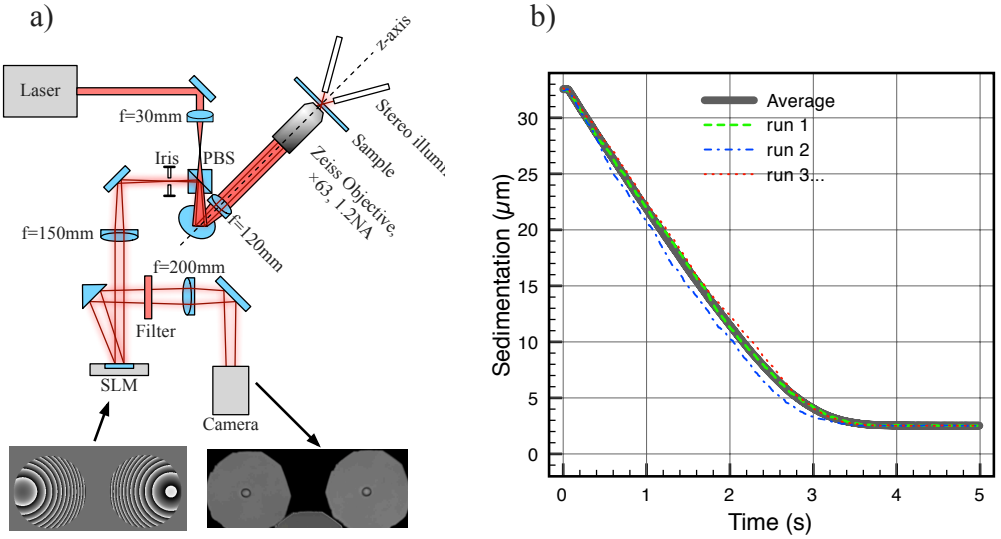

Fig. 1. a) Schematic view of the experimental setup. The red shaded area shows the path of the trapping laser, while the two red lines show the paths of the light from the two illumination fibres. The bottom-left image shows the SLM pattern that diffracts the light at a different angle for each illumination. The bottom-right image shows an example of a stereo image taken by the camera, from which the 3D position is obtained. b) The full position trace of a bead's centre recorded during sedimentation. The green (dashed), blue (dash-dot) and red (dot) lines show positions recorded from a single sedimentation run. We recorded up to 50 runs. The averaged result, shown in grey (solid line), is normalised with $z = 0$ being the bead on the coverslip, its centre being one particle radius higher. We measured this bead's diameter to be 4.84μm.

signal and the laser beam shut-off. This was measured by looking at laser light reflected by the coverslip and by adopting a very small region of interest such that the frame rate was greater than 1kHz. The calibration of the experiment starting time allowed us to determine exactly at which frame the laser was switched off; this being an important feature that relates to future microrheology measurements. The bead trajectory was measured by means of a video particle tracking procedure based on a centre of symmetry algorithm [20] applied separately to each view of the bead. Each view of the bead corresponds to a different viewing angle, meaning that the x positions measured on the camera are coupled to both x and z motion in the microscope. We can decouple the measurements on the camera to get the position of the bead in the microscope by taking the average of the two x measured positions (on the camera), and z position is given by $\mathrm{z} = \frac{\delta \mathrm{x}}{\tan\alpha}$, where δx is the difference between the two x measurements on the camera, and α is half angle between the fibres. The two y positions are the same on the camera (with some offset) as in the microscope, so we therefore have two independent measurements of y. As these coordinates are calculated in real time, we can then use the calculated z position to update the SLM with a Fresnel lens pattern, which refocusses the bead. We update the SLM at 100Hz. The linear relationship between Fresnel lens power and imaged focal height was empirically found. We achieved this by measuring the change in observed height of a bead adhered to the coverslip, moved by a known vertical distance with the translation stage. A scaling factor can then simply multiply the measured z displacement from the focal plane to

#203463 - $15.00 USD Received 19 Dec 2013; revised 6 Feb 2014; accepted 8 Feb 2014; published 20 Feb 2014

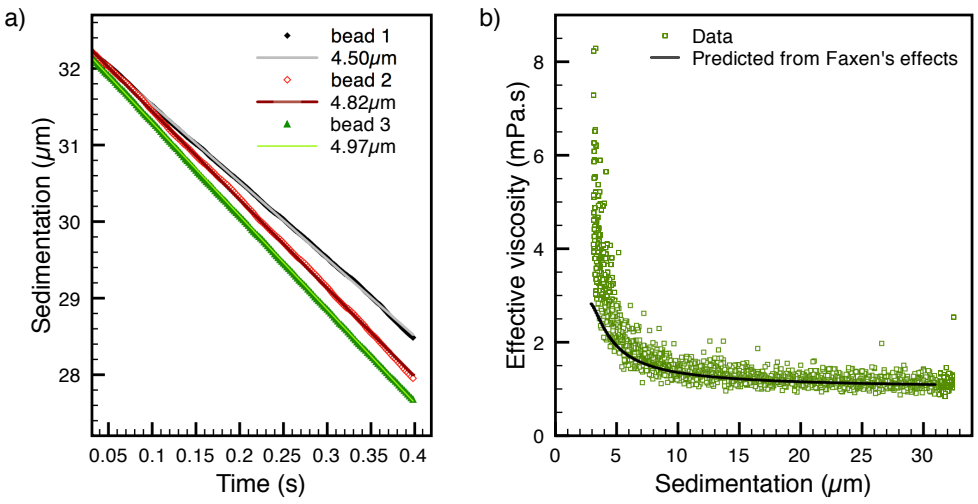

Fig. 2. a) The average initial part of sedimentation shown for three different beads. Over this range, the viscosity is nearly constant. With a linear fit, knowing the viscosity, we can extract the bead size or vice versa. b) The effective viscosity experienced by a sedimenting bead (diameter $= 4.84\mu$m) approaching a boundary.

obtain the focal length needed to refocus the image. Once the auto-focussing procedure has been calibrated, a bead remains in focus without adjustment of any optics. In principle, this procedure does not affect the position measurements described above, but only the precision of the measurement as the position of a more in focus bead suffers less from camera noise. In practice, as a bead goes out of focus, it may also obtain asymmetric distortions which will invalidate the centre of symmetry algorithm, i.e. the accuracy may also be more reliable for an in focus bead. In a previous work, we found that the lens correction procedure gave the position of a bead with an error of 5.5nm over a 50μm range [7].

3. Results

Typical z position traces are shown in Fig. 1(b). These data are from the same bead, and we average multiple sedimentations (up to 50 runs) to average out Brownian noise.

3.1. Particle sizing by sedimentation

The distance to the bounding coverslip decreases as the particle descends, resulting in the drag coefficient of the bead increasing according to Faxén's correction. However, during the initial part of the descent, from $32-28\mu$m, this effect is small, less than 1%. We therefore use this part of the trajectory to calculate the beads diameter. These measurements are shown in Fig. 2(a). The bead size is determined by fitting Eq. (1) to the data. Notably, Eq. (1) has a square dependence on the bead size, which enhances the sensitivity of the measurement. By averaging the measurements, the standard error in the bead sizing reduces to *circa* 1%. The parameters used in the fitting procedure are: a temperature of 22°C, density of silica of 2.0×10^3kg/m^3, density of water of 1.0×10^3kg/m^3 and water viscosity of 0.96mPa$\cdot$s.

#203463 - $15.00 USD Received 19 Dec 2013; revised 6 Feb 2014; accepted 8 Feb 2014; published 20 Feb 2014

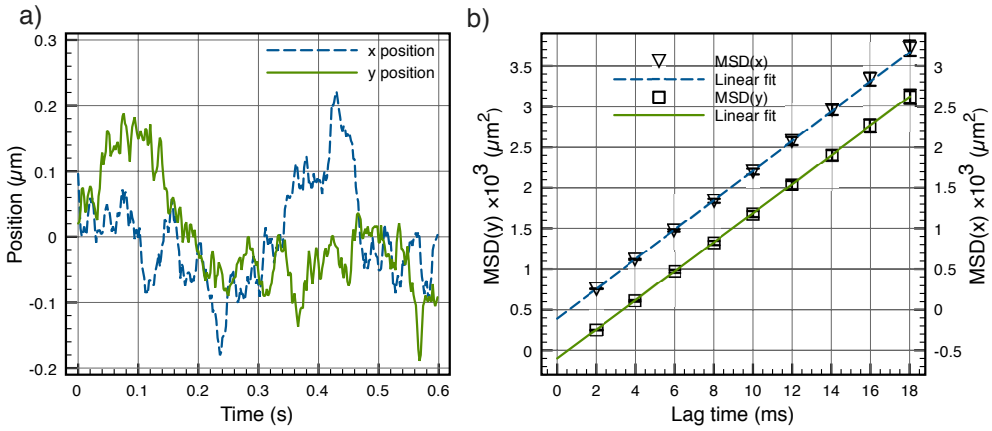

Fig. 3. During each sedimentation run, we also record the x and y position of the bead. Shown in a) is the x (blue, dashed) and y (green, solid) for an example run using a particle with diameter of 4.84μm. We then calculate the Mean Square Displacement (MSD) of this trajectory. By averaging the MSD for 50 repeats, we obtain the data shown in b). Here, the error bars are the standard error of the mean. The MSD(x) data ($\bigtriangledown$) from the MSD(y) data ($\square$) has been shifted for clarity. The fits do not intercept zero owing to the tracking error and finite exposure time in the acquisition [21]. From the slopes of the linear fits of MSD(x) (blue, dashed) and MSD(y) (green, solid) we obtain a particle size of 4.77μm and 4.90μm respectively

Table 1. Results comparing the diffusion method with the sedimentation method for particle sizing. The beads used come from a population with mean diameter of 4.72μm. For each particle, the standard deviation in sizes from the different methods is on average 3.5%.

	Sedimentation (μm)	$MSD(x)$ (μm)	$MSD(y)$ (μm)
Particle 1	4.50	4.51	4.81
Particle 2	4.82	5.28	5.06
Particle 3	4.97	4.66	4.73
Particle 4	4.95	4.93	4.60
Particle 5	4.88	5.07	4.71
Particle 6	4.86	4.99	4.77
Particle 7	4.53	4.85	4.52
Particle 8	4.84	4.77	4.90
Mean	4.79 ± 0.18	4.87 ± 0.22	4.74 ± 0.18

3.2. Particle sizing by diffusion

The particle tracking procedure is also able to provide the x and y coordinates. Far from the coverslip, these data are independent from the sedimentation process and therefore we can use them to estimate the bead size by means of its Mean Square Displacement (MSD) (computed as, in the x dimension, $\mathrm{MSD}(\vec{x}) = \left\langle [\vec{x}(t+\tau) - \vec{x}(t)]^2 \right\rangle$, where τ is the time interval or lag-time). For Newtonian fluids (e.g. water) the bead's MSD is expected to grow linearly with time, $\mathrm{MSD} = 2Dt$, where D is the diffusion coefficient given by $k_B T/6\pi\eta r$, where k_B is Boltzmann's constant and T is absolute temperature. Again, we are limited to only the initial part of the data

#203463 - $15.00 USD Received 19 Dec 2013; revised 6 Feb 2014; accepted 8 Feb 2014; published 20 Feb 2014

owing to the increase in drag coefficient closer to the coverslip. An example x and y position measurement is shown in Fig. 3(a), from which the MSD is calculated. We average the MSD for the many runs and fit to obtain the diffusion coefficient, Fig. 3(b). There exists an offset to the data which is due to a finite exposure time (2ms) and localisation error ($\sigma = 5$nm) [21]. Comparing the different methods (sedimentation and MSD) of finding bead size we find that the mean deviation between techniques is 3.5%. The overall size mean closely matches the given value from the manufacturer, Table 1. The MSD method is expected to be less reliable as the statistical averaging typically requires a long measurement, which is unavailable in this case as the bead is approaching the coverslip. Nonetheless, it provides additional information and acts as a good check that the system is calibrated.

3.3. Faxén's correction

In this section we show the Faxén's effect as manifest by a change in mobility experienced by a sedimenting bead. As the bead approaches the coverslip, the motion is still governed by the balance between the force due to gravity, buoyancy and surface friction. Experimentally, we observe the particle slowing down. This is a response to the increased friction coefficient.The change in mobility acts in the same way as change in effective viscosity $\eta(z)$, which can be found as a function of distance from the coverslip and is given by:

$$\eta(\mathrm{z}) = 2\mathrm{gr}^2(\rho_\mathrm{s} - \rho_\mathrm{f})/9\frac{\mathrm{dz}}{\mathrm{dt}}. \tag{2}$$

Using finite differences, we differentiate the 50 run average data shown in Fig. 1(b) to compute $\frac{\mathrm{dz}}{\mathrm{dt}}$, shown in Fig. 2(b). Using the bead size found previously we can calculate $\eta(\mathrm{z})$. The prediction is found from the equation for perpendicular Faxén's correction (with no free parameters) given in [15]. Owing to the numerical differentiation, the data is quite noisy (particularly close to the coverslip where the displacements are small), however there is a clear trend in agreement with theory.

4. Conclusion

We have demonstrated a new technique to measure the bead diameter and diffusion coefficient of microspheres by observing their sedimentation trajectory with a three dimensional SLM microscope. We used a closed-loop algorithm which automatically updates the SLM Fourier filter to increase the tracking range, allowing results to be recorded over both an initial range and while approaching a boundary. The bead diameter is found using the initial data, far from the coverslip using two methods: sedimentation and mean square displacement. We then use this result to find how Faxén's correction affects the sedimentation process and show good agreement with theory. We foresee our procedure to be of interest in the study of the sedimentation process itself, or in using sedimentation as a tool to study complex fluids.

Acknowledgments

MJP acknowledges support from the Royal Society. MT acknowledges support via personal research fellowship from the Royal Academy of Engineering/EPSRC.